

ABSTRACT

In Part 1, an extension of the theory of hydrogen-bond-dominated solids was proposed. In Part 2, the predictions of the extended theory are tested statistically using recently reported measurements of elastic moduli for 24 papers over a wide range of moisture contents. Moduli were reported both quasi-statically and ultrasonically. Statistical analysis shows that the effect of moisture in lowering the elastic modulus of paper is greater when the modulus is measured quasi-statically. The rate of decrease in the logarithm of modulus with moisture content when measured sonically is about 75% of the rate of decrease measured quasi-statically. The ratio of the two measured moduli for an isotropically equivalent paper is statistically indistinguishable from a ratio obtained from measurements of the effectiveness of water in reducing these elastic moduli. This supports one of the new predictions of the extended H-bond theory proposed in Part 1.

Application:

A model that predicts the effect of moisture content on elastic modulus.

IF THE ELASTIC MODULUS OF PAPER, E , is obtained from quasi-static measurements (indicated here by a subscript s) in a load-elongation test, then a relatively simple rule controls its value as the water content (mass of water per unit mass of paper), w , is changed. Above a critical water content, w_c , the negative value of $\partial \ln(E_s) / \partial w$ usually is a constant, which, in the terminology of the hydrogen-bond theory, is called the cooperative index, $CI_s(1)$. Similarly, if the modulus is measured by the speed of stress propagation on the same piece of paper using an ultrasonic method (indicated by a subscript u), one obtains a similar constant for $-\partial \ln(E_u) / \partial w = CI_u$ over a

Influence of water on the elastic modulus of paper

Part 2: Verification of predictions of the H-bond theory

STEFAN ZAUSCHER, DANIEL F. CAULFIELD, AND ALFRED H. NISSAN

very wide range of values of w , up to the fiber-saturation value. It is found (2-5) that CI_u is on the order of 0.5 CI_s to 0.75 CI_s . (Note that all variables are identified in the Nomenclature at the end of this article.)

In Part 1 of this paper (6), an explanation to resolve this apparent discrepancy was developed, based on the theory of hydrogen-bonded solids (1, 7-9). There, it was proposed that the modulus ratio at zero moisture content, E_0 , is predictable from values of the slope of $\ln E$ vs. w in Regime II and vice versa.

$$[(E_{0u}) / (E_{0s})]^3 = (CI_s + 1) / (CI_u + 1) \quad (1)$$

To arrive at this equation, it was postulated that the two values of E_0 obtained by ultrasonic and by quasi-static methods reflect two different forms of energy storage and propagation. Lacking the knowledge of the exact distribution of lengths, R , of the H-bonds and the density of effective H-bonds, n_e , in paper, an average value of $\langle k_R \rangle = 18.4$ N/m, as applying to both the ordered and the amorphous regions in cellulose, is adopted. It then can be assumed that all ordered regions have an equivalent H-bond density $(n_{equ})_u$, with a bond stiffness normalized to the average bond stiffness $\langle k_R \rangle$. Accordingly, all equivalent effective H-bonds (ordered and amorphous) average an H-bond density of $(n_{equ})_s$, and one obtains

$$[(E_{0u}) / (E_{0s})]^3 = [(n_{equu}) / (n_{equs})] > 1 \quad (2)$$

There is no theoretical prediction for how much the ratios exceed

unity. The ratios depend upon the morphology of the fibers, the manufacturing process, and the characteristic duration of the modulus measurement in each of the two methods. Thus, the difference between $(E_0)_u$ and $(E_0)_s$ arises from different types and densities of effective H-bonds activated in each of the two measurement methods.

To have an influence on E_s , a water molecule can interact with any H-bond to which it is accessible. But to affect E_u , it must effectively interact with an H-bond in a more ordered region, as, for example, at the surface of a crystallite. To achieve a critical water content in the ordered regions, more water is needed than predicted by $(w_c)_s$. For the present discussion, it is postulated that the critical water content is proportional to the equivalent H-bond density. The ratio of the equivalent H-bond densities is therefore equal to the ratio of critical water contents

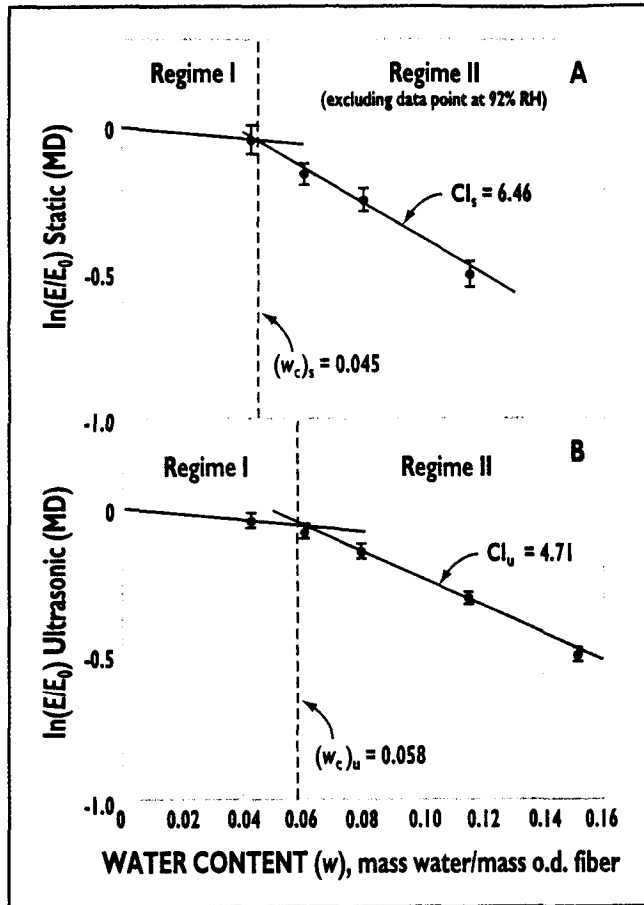
$$[(E_{0u}) / (E_{0s})]^3 = [(w_{cu}) / (w_{cs})] = \frac{[(n_{equu}) / (n_{equs})]}{[(n_{equu}) / (n_{equs})]} \quad (3)$$

From Eq. 3, using

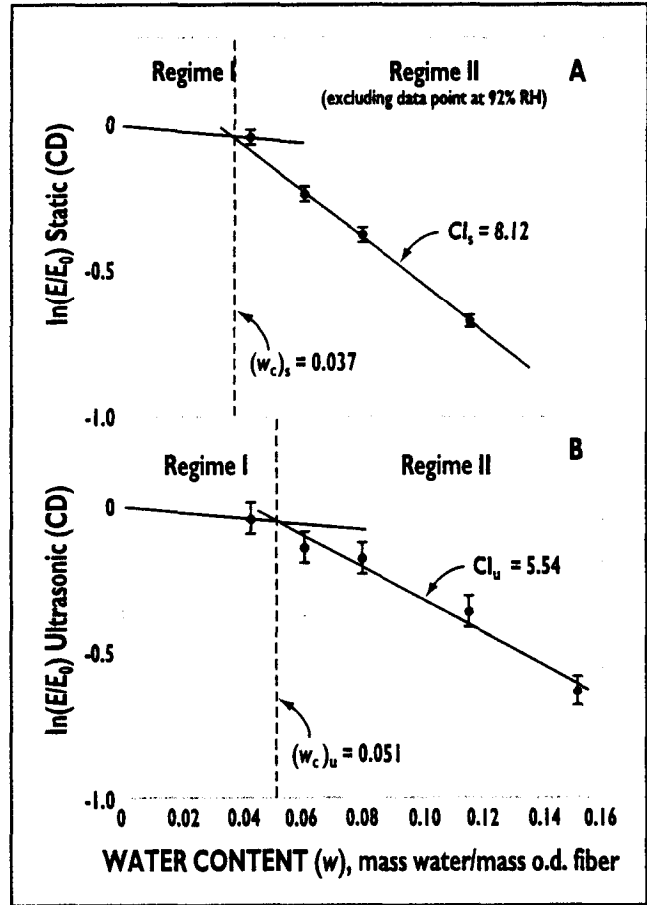
$$CI = (1/3w_c) - 1 \quad (4)$$

a relation from the H-bond theory, Eq. 1 is obtained.

Verification of this explanation was, not possible until recently because of the lack of a sufficiently large data set comprising modulus measurements by quasi-static and ultrasonic methods for a wide variety of papers over a wide range of



1. Specific modulus ratio $\ln(E/E_0)$ vs. water content w for Paper 11, an 89.1-g/m² linerboard from pine sulfate pulp. A: static measurements in MD; B: ultrasonic measurements in MD. (Data from Nordvall (10).)



2. Specific modulus ratio $\ln(E/E_0)$ vs. water content w for Paper 11, an 89.1-g/m² linerboard from pine sulfate pulp. A: static measurements in CD; B: ultrasonic measurements in CD. (Data from Nordvall (10).)

moisture contents. Nordvall (10) has recently provided this information for a set of 24 different papers, with modulus measurements taken in both machine direction (MD) and cross-machine direction (CD) over a relative-humidity range of 20% to 92%.

The objectives of the present work are

1. To use Nordvall's data as a basis for statistical evaluation of key predictions of the theory of hydrogen-bond-dominated solids pertaining to the discrepancy between ultrasonic and quasi-static moduli of paper
2. To explain the effect of water on paper modulus
3. To account for paper anisotropy.

NORDVALL'S DATA

Nordvall (10) provides ultrasonic and static modulus measurements obtained from a set of 24 different papers in the MD and CD. To utilize this extensive set of data for our purpose, it is first necessary to test the agreement of the H-bond theory with the reported quasi-static data. If this agreement is satisfactory, ultrasonic measurements can be analyzed in much the same way.

Considering Nordvall's data, there are two limitations related to

1. Density dependence
2. Modulus values for the dry state.

Values for moduli are reported only as specific moduli, E , i.e., the modulus divided by the apparent

density of the paper sample at the time of test. This means that $\partial E/\partial w$ and $\partial \ln(E)/\partial w$ differ from $\partial E/\partial w$ and $\partial \ln(E)/\partial w$ by terms of $\partial \rho/\partial w$ and $\partial \ln(\rho)/\partial w$, respectively. The use of specific moduli does not alter the predictions of the H-bond theory under the assumption that the apparent paper densities do not change much with increasing moisture content. In other words, for the range of w in Nordvall's paper samples, the terms $\partial \rho/\partial w$ and $\partial \ln(\rho)/\partial w$ are small. A 3.9% decrease in apparent density of linerboard, reported by Baum *et al.* (3), in the range from 20% RH to 80% RH ($0.045 < w < 0.145$), may serve as an estimate of the magnitude of such terms. This means that at higher moisture contents, the true modulus is higher

Data set ^a	Sample size	Cooperative index (CI)		CI _u /CI _s	Critical water content (w _c), %			
		Static	Ultrasonic		Static	Ultrasonic	(CI _s +1)/(CI _u +1) [(E _{0u})/(E _{0s})] ²	
1	24	7.33 ± 1.50	5.46 ± 0.92	0.74	4.14 ± 0.80	5.25 ± 0.70	1.29 ± 0.17	1.17 ± 0.27
2	23	8.84 ± 1.96	6.94 ± 1.49	0.78	3.51 ± 0.66	4.33 ± 0.76	1.23 ± 0.16	1.56 ± 0.39
3	23	8.09 ± 1.54	6.20 ± 0.89	0.77	3.77 ± 0.63	4.70 ± 0.57	1.26 ± 0.14	1.34 ± 0.27
4	23	7.89 ± 1.46	6.01 ± 0.78	0.76	3.85 ± 0.63	4.81 ± 0.53	1.26 ± 0.14	1.30 ± 0.27

^aData are presented as averages with standard deviation
^bSet 1, MD data only; Set 2, CD data only; Set 3, geometric mean of MD and CD data; Set 4, modified geometric mean of MD and CD data.

I. Summary of results for Sets 1-4^a

Data set ^a	Significant at α = 0.05	p-value	Probability of determining a difference of X% between ratios				
			5%	10%	15%	20%	25%
1	No	0.156	0.11	0.29	0.56	0.80	0.94
2	Yes	0.004
3	No	0.287	0.14	0.40	0.72	0.92	0.99
4	No	0.638	0.13	0.39	0.71	0.92	0.99

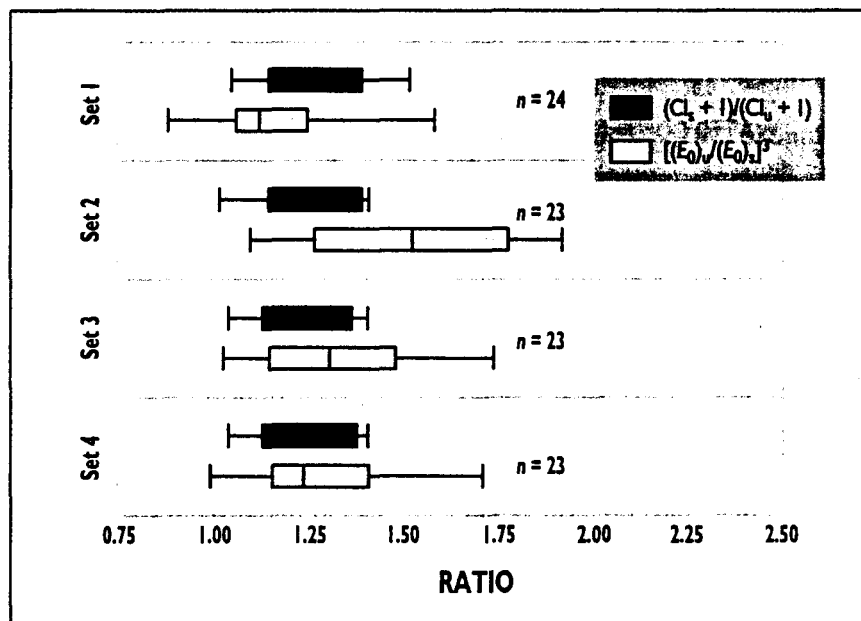
^aSet 1, MD data only; Set 2, CD data only; Set 3, geometric mean of MD and CD data; Set 4, modified geometric mean of MD and CD data.

II. Significance test for the difference between (CI_s + 1)/(CI_u + 1) and [(E_{0u})/(E_{0s})]²

than the one obtained from an uncorrected specific modulus. In the following, the specific moduli, E, will be denoted just by E to avoid an excessive number of superscripts.

No modulus measurements are available for the 24 papers in the oven-dry state. Values for E₀ were therefore estimated from the predictions of the H-bond theory. This allows therefore only a test of the internal consistency of the proposed extension to the H-bond theory.

The quasi-static modulus values at high relative humidity present some difficulties. Nordvall (10) reported that it was not possible to measure accurately static moduli at 92% RH, even though the coefficient of variability for static modulus measurements at 92% RH is not much out of line with those at lower levels of RH. However, the quasi-static modulus values at 92% RH were consistently lower than expected. In contrast, Nordvall (10) reported no similar difficulties with the ultrasonic measurements at 92% RH. In order to be confident that paper modulus is determined strictly by the intermolecular force contributions to cohesive energy density, the glassy state of the wood polymers in paper is required.



3. Comparison of (CI_s + 1)/(CI_u + 1) and [(E_{0u})/(E_{0s})]² for Sets 1-4. Data are presented in the form of box-and-whisker plots, with the box representing the interquartile range (25% to 75%) and the median displayed within.

At temperatures above the glassy states, entropic contributions to cohesive energy density may become significant.

A very pronounced thermal transition in wood polymers is associated with the α-relaxation. This relaxation can be thought of as corresponding to the glass-transition in

these polymers. Plasticizers, such as water for wood polymers, shift the isofrequency modulus curves and damping peaks to lower temperatures (11-13), i.e., increasing moisture content shifts the isothermal modulus-frequency response toward higher frequencies. The thermal dispersion region is broadened

RH, %	w, %	E_{un}^{*b} MN·m/kg	E_{un}^{*n} MN·m/kg	$E_c^* = 0.5(E_{un}^{*b} + E_{un}^{*n})$ MN·m/kg	E_{un}^{*b} MN·m/kg
20	4.23	13.66 ± 0.71	13.80 ± 0.65	13.73 ± 0.48	14.54 ± 0.15
40	6.04	12.57 ± 0.26	13.20 ± 0.27	12.89 ± 0.19	14.29 ± 0.14
60	7.95	11.36 ± 0.39	12.26 ± 0.47	11.81 ± 0.30	13.37 ± 0.13
78	11.50	8.26 ± 0.35	9.97 ± 0.42	9.12 ± 0.27	11.36 ± 0.11
92	15.15	2.95 ± 0.14	3.09 ± 0.14	Excluded	9.33 ± 0.09

*Original data from Nordvall (10) are in bold type; calculated data are in normal type.
^bStandard deviation based on assumed 1% error.

A-I. Original data for Paper 11, machine direction^a

RH, %	w, %	E_{un}^{*b} MN·m/kg	E_{un}^{*n} MN·m/kg	$E_c^* = 0.5(E_{un}^{*b} + E_{un}^{*n})$ MN·m/kg	E_{un}^{*b} MN·m/kg
20	4.23	4.98 ± 0.15	4.87 ± 0.19	4.93 ± 0.12	5.91 ± 0.05
40	6.04	4.86 ± 0.14	4.86 ± 0.17	4.86 ± 0.11	5.50 ± 0.06
60	7.95	4.16 ± 0.16	4.24 ± 0.15	4.20 ± 0.04	5.29 ± 0.05
78	11.50	2.92 ± 0.05	3.33 ± 0.07	3.13 ± 0.04	4.39 ± 0.04
92	15.15	0.87 ± 0.05	0.92 ± 0.04	Excluded	3.35 ± 0.03

*Original data from Nordvall (10) are in bold type; calculated data are in normal type.
^bStandard deviation based on assumed 1% error.

A-II. Original data for Paper 11, cross-machine direction^a

with increasing amount of plasticizer added (11, 12). Salmén (14) reports a reduction in the glass-transition temperature (T_g) for hemicelluloses from temperatures of 160-200°C in the dry state to below 0°C at moisture contents above 30%. For the disordered regions of cellulose, T_g is lowered from about 230°C to 90°C over the same moisture range. A similar reduction in T_g is reported for lignin.

At the highest humidity of Nordvall's static modulus measurement (92% RH), paper—especially papers with significant levels of hemicelluloses and lignin—may be plasticized enough so that, during slow mechanical straining, relaxation phenomena characteristic of glass transitions may begin to contribute significantly to paper modulus (12, 13). And although the moisture conditions and the temperatures needed for the onset of these transitions are not well defined, their possible influence would be greatest at higher humidities and the longer stress durations in quasi-static measurements.

For these two reasons—Nordvall's dissatisfaction with the accuracy of 92% RH static measurements, and the suggestion that other modes

of stress relaxations may be participating—we feel it is best to limit the static modulus data to those under 92% RH for the present analysis. All but one measurement series (Paper 21 in the CD) have been used in the present data analysis. The calculated value for CI in Paper 21 (10) deviates from the mean of all others by more than four standard deviations, so the corresponding data were omitted.

To improve the accuracy of the calculations, some of the considerations discussed by Batten (15) and presented in Part 1 of this paper (6) should be accounted for. A small adjustment of the moduli arises by accounting for the two different thermodynamic regimes [adiabatic, nonadiabatic (isothermal)] under which the two modulus measurements were obtained. This requires knowledge of the specific heat at constant pressure, c_p , for each paper (15). This information was not available for Nordvall's papers. An overestimate of the ultrasonic moduli arises from use of the low-frequency approximation (15.). The low-frequency approximation posits that below a critical frequency (≈ 100 kHz), the longitudinal waves travel-

ing in the plane of the paper do not induce out-of-plane (z -directional) motion, i.e., plane stress analysis is sufficient to describe the state of stress in paper. A more accurate sonic modulus can be obtained if out-of-plane elastic constants are known. However z -directional stiffness coefficients are not routinely measured and are not available for the present analysis.

TAKING PAPER ANISOTROPY INTO ACCOUNT

To compare elastic moduli of papers with different degrees of anisotropy, an "invariant" modulus is useful. Furthermore, the equations for the H-bond theory, as developed in Part 1 of this paper (6), are strictly only valid for an isotropic material.

The shear modulus of orthotropic materials can be calculated from the isotropic elastic modulus and the isotropic Poisson ratio, both of which are approximated by a geometric mean of the respective values in the principal directions. Using this method, excellent agreement between the measured and the derived shear modulus has been found (3). Similarly, Htun and Fellers (16) proposed a geometric mean as an invari-

Regime	w, %	STATIC		ULTRASONIC	
		$E_s^* = 0.5(E_{wb}^* + E_{cd}^*)$, MN·m/kg	$\ln E_s^*$	E_u^* , MN·m/kg	$\ln E_u^*$
I	4.23	13.73 ± 0.48	2.62 ± 0.03	14.54 ± 0.15	2.68 ± 0.01
II	6.04	12.89 ± 0.19	2.56 ± 0.01	14.29 ± 0.14	2.66 ± 0.01
II	7.95	11.81 ± 0.30	2.47 ± 0.03	13.37 ± 0.13	2.59 ± 0.01
II	11.50	9.12 ± 0.27	2.21 ± 0.03	11.36 ± 0.11	2.43 ± 0.01
II	15.15	Excluded	Excluded	9.33 ± 0.09	2.23 ± 0.01

A-III. Set 1, machine direction, Paper 11

	A	CI	r ²	w, %	(E _s [*]) ⁿ , MN·m/kg	[(E _s [*]) ⁿ /(E _u [*]) ⁿ] ^{1/2}	(CI _s +1)/(CI _u +1)
Static	2.96 ± 0.03	6.46 ± 0.70	0.99	4.47 ± 0.42	15.13 ± 0.43		
Ultrasonic	2.96 ± 0.02	4.71 ± 0.25	0.99	5.84 ± 0.25	15.50 ± 0.28	1.08 ± 0.42	1.31 ± 0.13

Data in bold type were combined with similar data for 23 other papers from Nordvall's work (10) in calculating Set 1 in Table I.

A-IV. Set 1, regression in Regime II for Paper 11 (MD); $\ln(E^*)^n = A + [(-1)CI \cdot w]$

Regime	w, %	STATIC		ULTRASONIC	
		$E_s^* = 0.5(E_{wb}^* + E_{cd}^*)$, MN·m/kg	$\ln E_s^*$	E_u^* , MN·m/kg	$\ln E_u^*$
I	4.23	4.93 ± 0.12	1.59 ± 0.02	5.91 ± 0.06	1.78 ± 0.01
II	6.04	4.86 ± 0.11	1.58 ± 0.02	5.50 ± 0.06	1.70 ± 0.01
II	7.95	4.20 ± 0.11	1.44 ± 0.03	5.29 ± 0.05	1.67 ± 0.01
II	11.50	3.13 ± 0.05	1.14 ± 0.01	4.39 ± 0.04	1.48 ± 0.01
II	15.15	Excluded	Excluded	3.35 ± 0.03	1.21 ± 0.01

A-V. Set 2, cross-machine direction, Paper 11

ant of the specific modulus of paper when it is dried under the same conditions

$$E_{iso}^* = (E_{MD}^* E_{CD}^*)^{1/2} \quad (5)$$

Batten and Nissan (17, 18) derived an invariant modulus invoking the structural theory of paper by Perkins and Mark (19) by introducing an orientation correction factor, *d*, in Eq. 5, such that

$$E_{iso}^* = (d E_{MD}^* E_{CD}^*)^{1/2} \quad (6)$$

where

$$d = (36 - a_1^2)/[9(4 - a_1^2)] \quad (7)$$

and

$$a_1 = \{[4(r+1)] - \{2[(r^2+14)/(r+1)]^{1/2}\}/(r-1)\} \quad (8)$$

with the anisotropy ratio

$$r = E_{MD}^*/E_{CD}^* \quad (9)$$

The correction factor, *d*, is derived by making the simplifying assumptions that the in-plane fiber orientation in a sheet of paper is elliptical and that the sheet is biaxially restrained during drying. However, there has been some controversy in the literature on the meaning of "invariant" properties of anisotropic sheets (20, 21).

To evaluate the influence of paper anisotropy, four data sets were prepared for the present study. Sets 1 and 2 use MD and CD measurements, respectively. Sets 3 and 4 attempt to

take modulus anisotropy into account. Set 3 reflects the geometric mean of *E_{MD}*^{*} and *E_{CD}*^{*} (Eq. 5) (16), and Set 4 was derived from Set 3, forcing the geometric mean into invariance by including the orientation factor *d* (Eqs. 6-9) (17, 18). No new information is gained if an invariant modulus is derived for either Set 1 or 2, because the results will be identical to those from Set 4. The Appendix shows how the data for Sets 1-4 were derived for one of the papers (Paper 11) studied in Nordvall's work (10). Data for all other papers were calculated analogously.

FITTING THE H-BOND THEORY TO NORDVALL'S DATA
Nordvall (10) used two different methods—triangulation and fit to two-parameter hyperbolic sine

	A	CI	r ²	w, %	(E ₀ ^u) ³ , MN·m/kg	[(E ₀ ^u) _u /(E ₀ ^s) _s] ³	(CI _s +1)/(CI _u +1)
Static	2.07 ± 0.01	8.12 ± 0.18	1.00	3.66 ± 0.07	6.14 ± 0.04	1.10 ± 0.41	1.39 ± 0.15
Ultrasonic	2.08 ± 0.05	5.54 ± 0.69	0.97	5.10 ± 0.54	6.34 ± 0.31		

Data in bold type were combined with similar data for 22 other papers from Nordvall's work (10) in calculating Set 2 in Table I.

A-VI. Set 2, regression in Regime II for Paper 11 (CD); $\ln(E^u)^3 = A + [(-1)CI \cdot w]$

Regime	w, %	STATIC		ULTRASONIC	
		E ₀ ^u = 0.5(E ₀ ^u + E ₀ ^s), MN·m/kg	ln E ₀ ^u	E ₀ ^s , MN·m/kg	ln E ₀ ^s
I	4.23	8.22 ± 0.18	2.10 ± 0.02	9.27 ± 0.07	2.23 ± 0.01
II	6.04	7.91 ± 0.11	2.07 ± 0.01	8.87 ± 0.06	2.18 ± 0.01
II	7.95	7.04 ± 0.13	1.95 ± 0.02	8.41 ± 0.06	2.13 ± 0.01
II	11.50	5.34 ± 0.09	1.67 ± 0.05	7.06 ± 0.05	1.95 ± 0.01
II	15.15	Excluded	Excluded	5.59 ± 0.04	1.72 ± 0.01

A-VII. Set 3, geometric mean, Paper 11

	A	CI	r ²	w, %	(E _{0,geo} ^u) ³ , MN·m/kg	[(E _{0,geo} ^u) _u /(E _{0,geo} ^s) _s] ³	(CI _s +1)/(CI _u +1)
Static	2.52 ± 0.02	7.29 ± 0.44	1.00	4.02 ± 0.21	9.63 ± 0.17	1.09 ± 0.39	1.35 ± 0.13
Ultrasonic	2.52 ± 0.03	5.13 ± 0.47	0.98	5.44 ± 0.42	9.91 ± 0.33		

Data in bold type were combined with similar data for 22 other papers from Nordvall's work (10) in calculating Set 3 in Table I.

A-VIII. Set 3, regression in Regime II for Paper 11 (geometric mean); $\ln(E^u)^3 = A + [(-1)CI \cdot w]$

model (22) —to evaluate the modulus obtained from mechanical tests. In the present work, the arithmetic average of the measurements from each method is used. Similar variances in each method justify this approach. Modulus values at 20% RH are always assumed to belong to Regime I and are excluded from the regression analysis for Regime II. A typical fit to static modulus data of one of the papers (Paper 11, 89.1-g/m² linerboard from pine sulfate pulp (10)) is represented in Fig. 1a for the MD and Fig. 2a for the CD. The full calculation for Paper 11, representative for all papers, is given in the Appendix.

The fit of data to the equations of the H-bond theory can be gauged in

several ways. Good agreement with the predictions of Eq. 10

$$\ln[E_{(w)}^u/E_0^u]^3 = D - (CI \cdot w) \quad (10)$$

and the validity of Eq. 11

$$\ln E_0^1 = \ln E_0^u \quad (11)$$

can serve as a check. In the present case, in E₀¹ has a large uncertainty associated with it because an insufficient amount of data in Regime I precluded a regression analysis. The following analysis was therefore based on the prediction of E₀ from observations in Regime II alone.

The predictions of the H-bond theory for the difference in the slope values of $\ln E_{(w)}^u$ vs. w was tested statistically using a hypothesis test. The

hypothesis to be tested (null hypothesis, H_0) was that the equality in Eq. 1 holds, i.e., that there is no difference between the ratios of $(CI_s + 1)/(CI_u + 1)$ and $[(E_0^u)_u/(E_0^s)_s]^3$. The acceptance of H_0 merely implies that the data do not give sufficient evidence to refute it. On the other hand, rejection implies that the sample evidence refutes it. The probability of rejecting H_0 when it is true is called the level of significance, α . The alternative hypothesis (H_1) was assumed to be two-sided. That means the critical region for H_1 lies with equal probabilities in each tail of the distribution of the test statistic.

Because static and ultrasonic measurements of modulus for each of the 24 papers were performed on

the same experimental unit (i.e., a particular paper type), these measurements are considered paired. Statistical inferences from these measurements were therefore considered to be derived from observations that are not independent. Under the assumption that observations from each population are normally distributed, and considering a maximal sample size of 24, the *t*-distribution was chosen as the test statistic. In the present study, the *i*th pair consisted of the observation

$$d_i = [(CI_s + 1)/(CI_u + 1)]_i - [(E_0)_u/(E_0)_s]_i^3 \quad (12)$$

Under the null hypothesis that the equality of Eq. 1 holds and a two-sided alternative hypothesis, a critical region for *t* (*t* < *t*_{ω2} and *t* > *t*_{ω2}) with *n*-1 degrees of freedom was calculated with

$$t = \langle d \rangle / (s_d / n^{1/2}) \quad (13)$$

where $\langle d \rangle$ and s_d are, respectively, the mean and the standard deviation of the normally distributed differences of *n* pairs of observations. If this calculated *t* value fell in the critical region, the null hypothesis was rejected, and it was concluded that the difference between the populations, i.e., the ratios, is significant at the chosen level of significance.

RESULTS AND DISCUSSION

Numerical results for the four data sets (MD, CD, geometric mean, modified geometric mean) are summarized in **Tables I and II**. Data in Table I reflect the average and standard deviation for some of the key variables derived for each set. Results of the statistical tests are summarized in Table II, where a *p*-value indicates the lowest level of significance at which the observed value of the test statistic was significant. To determine how sensitive the statistical test was in detecting differences between the ratios (power of the test), the probability for detecting a 5%, 10%, 15%, 20%, and 25% difference is tabulated for the cases where the difference was not significant at the 0.05 level (Table II). The ratio of $(CI_s + 1)/(CI_u + 1)$ is compared with the ratio of $[(E_0)_u/(E_0)_s]^3$ in the form of a box-and-whisker plot for each set in **Fig. 3**. These ratios were predicted to be equal, based on the extension of the hydrogen-bond theory presented in Part 1 of this paper (6). The plots in Fig. 3 enclose the interquartile range of the data in a box that has the median displayed within. Thus, the center of location, the variability, and the degree of asymmetry in the data become apparent.

Fit of data

The values for $\ln E_0^u$ were generally greater than those for $\ln E_0^s$ although, according to Eq. 11, their values should have been equal. This discrepancy is most likely due to lack of experimental data in Regime I, where a slope of -1 had to be assumed for the calculation of $\ln E_0^s$.

The *CI_s* values for all data sets are greater than the experimentally found average of previously reported values, 6.7 (1). *CI_u* values are, with exception of Set 2, even smaller than a theoretically derived value of 6.4 (9).

Regression analysis of ultrasonically measured moduli in Regime II yielded straight lines with slopes less than those for

Regime	w, %	STATIC				ULTRASONIC				
		$r_{MD}^u/(E_{CD})_u$	$(a_1)_u$	d_u^b	$[d_u(E_{MD})_u(E_{CD})_u]^{0.5} / MN \cdot m/kg$	$(E_{MD})_u^2 / (E_{CD})_u$	$(a_1)_u^d$	d_u^e	$[d_u(E_{MD})_u(E_{CD})_u]^{0.5} / \ln(E_{MD})_u$	
I	4.23	2.79	0.74	1.14	8.78 ± 0.16	2.17 ± 0.02	2.46	1.11	9.75 ± 0.06	2.28 ± 0.01
II	6.04	2.65	0.70	1.13	8.40 ± 0.10	2.13 ± 0.01	2.60	1.12	9.39 ± 0.06	2.24 ± 0.01
II	7.95	2.81	0.75	1.14	7.53 ± 0.12	2.02 ± 0.02	2.53	1.11	8.88 ± 0.06	2.18 ± 0.01
II	11.50	2.92	0.77	1.15	5.74 ± 0.08	1.75 ± 0.01	2.59	1.12	7.47 ± 0.05	2.01 ± 0.01
II	15.15	Excluded	Excluded	Excluded	Excluded	Excluded	2.79	1.14	5.97 ± 0.04	1.77 ± 0.01

^a $(a_1)_u = ((4(r_u + 1)) - (2[(r_u^2 + 14)(r_u + 1)]^{0.5}))/r_u - 1$
^b $d_u^b = [36 - (a_1)_u^2]/9 [4 - (a_1)_u^2]$
^c Error propagation same as for geometric mean in Set 3
^d $(a_1)_u = ((4(r_u + 1)) - (2[(r_u^2 + 14)(r_u + 1)]^{0.5}))/r_u - 1$
^e $d_u^e = [36 - (a_1)_u^2]/9 [4 - (a_1)_u^2]$

A-IX. Set 4, modified geometric mean, Paper 11

	A_s	CI	r^2	w_s %	$(E_{0,low})^4$, MN·m/kg	$[(E_{0,low})_s/(E_{0,low})_p]^3$	$(CI_s+1)/(CI_p+1)$
Static	2.57 ± 0.02	7.08 ± 0.50	1.00	4.13 ± 0.27	10.13 ± 0.20	1.09 ± 0.37	1.34 ± 0.12
Ultrasonic	2.57 ± 0.03	5.02 ± 0.42	0.99	5.53 ± 0.38	10.41 ± 0.31		

Data in bold type were combined with similar data for 22 other papers from Nordvall's work (10) in calculating Set 4 in Table I.

A-X. Set 4, regression in Regime II for Paper 11 (modified geometric mean); $\ln(E_{0,low})^4 = A + [(-1)CI \cdot w]$

the static measurements (see Table I and, as an example, Figs. 1b and 2b) and r^2 values usually greater than 0.99. Within each of the four data sets, the difference between static and ultrasonic CI values was statistically highly significant. This suggests that there is a difference between the CI values obtained from static and ultrasonic measurements for the present data. The constant CI_s/CI_p ratio of about 0.75 for all four sets (Table I) is in good agreement with reported values (2, 3).

Given the insufficient number of data points at low water contents, the existence of a Regime I for ultrasonic measurements could not be proven rigorously. Data from Caulfield and Weatherwax (4), however, lend some support to the existence of a Regime I for sonic measurements, although these researchers extended Regime II to the y-intercept.

The results confirm the difference and the magnitude of difference between slope values of $\ln E$ vs. w for the static and sonic measurements found by other researchers, and the present results agree with the predictions of the H-bond theory quite well, considering the limitations of the data.

Paper anisotropy

Quantitative predictions of the H-bond theory should be valid only for isotropic papers. A qualitative discussion is nonetheless useful.

The cooperative index, CI, is a direct measure of the influence of water on elastic modulus. If this value is small, the loss in stiffness with increasing moisture content is small. If the value is large, the loss in

stiffness is large. It is remarkable that the effect of water on stiffness loss is constant over the moisture range in the present data, as expressed by the constant cooperative index in Table I. Considering CI values from Sets 1 and 2 (Table I), it is apparent that moisture-induced stiffness loss in MD is less than that in CD.

Paper anisotropy can explain this dependence of CI on direction or, in other words, the directional sensitivity of stiffness on moisture content. Anisotropy arises from preferred fiber alignment in the machine direction and drying restraints during the papermaking process. On the fiber level, anisotropy is caused by the relatively low fibril angle of cellulose microfibrils in the S2 layer of the fiber cell wall. Furthermore, pulp fibers consist not only of cellulose but also of hemicellulose and lignin in varying amounts. In a simplified structural model, ignoring the contribution of lignin, a single pulp fiber can be viewed as having parallel structural elements made from low-stiffness hemicelluloses and high-stiffness cellulose. The cellulose element can be further regarded as a series model of amorphous and crystalline cellulose components. This simplified model illustrates that the influence of moisture on fiber elastic modulus is dependent on the individual responses of the coupled elements in the system. The parallel coupling of hemicelluloses minimizes their contribution to overall stiffness loss as a function of increasing moisture content in the fiber-length axis. Thus, as a function of moisture content, hemicelluloses—and lignin—exert a stronger influ-

ence on fiber and, ultimately paper elasticity in the cross-fiber direction (14). Stiffness is lower in this cross-fiber direction. The serial coupling of amorphous and crystalline components in the cellulose element makes the fiber elastic modulus along the fiber axis sensitive to moisture-induced stiffness changes in the amorphous regions.

The present data support this argument, in that moisture affects stiffness in the CD more than in the MD. In terms of the H-bond theory (derived for an isotropically hydrogen-bonded solid), this means that it is necessary to derive an invariant, isotropic modulus to account for paper anisotropy. In the present analysis, this was most successfully accomplished in Set 4, using Eqs. 6-9. Accounting for paper anisotropy markedly improved the agreement between the ratios in Eq. 1 and is reflected by a large p -value for Set 4 (Tables I and II and Fig. 3).

Verification of Eq. 1

The significance test for the difference between the ratios of $(CI_s+1)/(CI_p+1)$ and $[(E_{0,low})_s/(E_{0,low})_p]^3$ reveals, using predicted $E_{0,low}$ values derived from Regime II only, that the difference between the ratios is statistically not significant for Sets 1, 3 and 4 (Tables I and II) at an α level of 0.05. A p -value of 0.64 for Set 4, by far the highest, indicates that one can be very confident in accepting the null hypothesis that there is no difference between the ratios. The power of the test to detect differences in the ratios indicates that for Set 1, one can be confident that there is not a 25% difference. If there had been a 25% difference, one

KEYWORDS

Anisotropy, elastic strength, forecasts, hydrogen bonds, load elongation, logarithms, measurement, moisture content, paper, paper tests, solids content, theories, ultrasonic tests, water.

would have a high probability (0.94) in detecting it. Similarly, for Set 3 and 4, the probability in detecting a 20% difference would be 0.92. Best concordance with the null hypothesis, i.e., that Eq. 1 holds, are obtained for Set 4. In this set, paper anisotropy is accounted for by using an invariant modulus as derived in Eqs. 6-9. This is in line with the H-bond theory, which is derived for isotropic hydrogen-bonded solids.

Figure 3 shows the modulus ratios and the slope ratios in the form of box-and-whisker plots for Sets 1-4. The asymmetric position of the median line in the boxes indicates some degree of asymmetry in the data. While the overall spread in the data is lower for Sets 3 and 4, the interquartile range is smallest for Set 1. It is believed that the reduction in the spread of the data arises from taking paper anisotropy into account.

These results, cast in the terminology of the H-bond theory, suggest that the number density of effective H-bonds in ultrasonic measurements, normalized to an average H-bond stiffness of $\langle k_r \rangle = 18.4$ N/m, is larger than the equivalent number density of effective bonds for static measurements. Theory indicates that the ratio of these equivalent H-bond densities can be predicted from the ratio of the critical water content for ultrasonic and static measurements. This ratio, in turn, can be obtained from the magnitude of slope values of $\ln E$ vs. w for each of the two measurement methods. Thus, the postulate that different types and numbers of H-bonds are activated, dependent on the type of modulus measurement, appears to

be confirmed within the limitations of the data. The difference in the slope values of $\ln E$ vs. w for ultrasonic and static modulus measurements can therefore be explained by the extension to the H-bond theory.

CONCLUSIONS

Analysis of Nordvall's data (10) indicates that there is a difference between elastic modulus measured by quasi-static and ultrasonic methods on the same paper sample. This difference can be explained by the view that there exist two different forms of energy storage and propagation in cellulose, dependent on the method of modulus measurement.

The present analysis shows that paper anisotropy can be taken into account by a modified geometric mean of the modulus values in the MD and CD. The different slopes of $\ln E$ vs. w for the MD and CD can then be explained by a mechanistic model in which stiff and soft, water-accessible domains of a pulp fiber are coupled in series and parallel and oriented in the plane of the paper. Stiffness in CD is less than in MD, and the effect of water on stiffness is stronger in the CD, as evidenced by a greater slope of $\ln E$ vs. w in this direction.

The present data analysis suggests that, despite the limitations in the available data, the H-bond theory can be extended to explain and predict the apparent discrepancies quantitatively. This extension states that the equivalent number density of effective H-bonds (H-bonds normalized to an average H-bond with a bond stiffness of $\langle k_r \rangle = 18.4$ N/m) is higher for ultrasonic measurements than it is for static measurements. The ratio of these numbers can be predicted from the ratio of the slopes of $\ln E$ vs. w in Regime II, i.e., from the values of CI (cooperative index). Other theories or explanations for the changes in modulus due to moisture—such as plasticization, free-volume, or cohesive energy density—may be qualitatively identi-

cal, but they are not amenable to similar quantitative verification.

Table I shows that $[(E_u)/(E_s)]^3 \approx 1.3$. This means that there is just about a 10% difference between ultrasonic and static moduli. This difference at zero moisture content may be difficult to discern, considering the uncertainties involved in the two measurement methods. Nevertheless, the significant difference in CI values indicates that, in general, at nonzero moisture contents, the differences between E measured quasi-statically and E measured ultrasonically are real and reflect water's different roles in the dispersion and dissipation mechanisms of energy storage and propagation. Careful measurements at zero moisture content—accounting for thermodynamic differences in the measurements, the low-frequency approximation, and paper viscoelasticity—are needed to confirm if the approximate 10% difference at zero moisture content is real or if it arises from the extrapolation assuming the H-bond theory.

Although the present work focuses on paper, similar analyses should hold for other hydrogen-bond-dominated solids. An analysis of modulus-water interactions for hydrogen-bonded solids other than paper may, in the future, serve as an independent check of the proposed explanation. **TJ**

Zauscher is a graduate student in the materials science program at the University of Wisconsin, 1415 Engineering Drive, Madison, WI 53706. Coulfield is a research chemist, USDA Forest Products Laboratory, One Gifford Pinchot Dr., Madison, WI 53705-2398. Nissan is a consultant, 6A Dickel Rd., Scarsdale, NY 10583-2118.

The authors are grateful to E Nordvall and C. Fellers from the Royal Institute of Technology in Stockholm, Sweden. Their data made this analysis possible. The help in statistical matters by S. Verrill of the USDA Forest Products Laboratory, Madison, WI, is greatly appreciated.

Received for review Nov. 18, 1995.

Accepted April 4, 1996.

LITERATURE CITED

1. Nissan, A. H., *Lectures on Fiber Science in Paper, Pulp and Paper Technology Series*, No. 4, Joint Textbook Committee of the Paper Industry, TAPPI PRESS, Atlanta, and CPPA, Montreal, 1977.
2. Weatherwax, R. C. and Caulfield, D. F., *Tappi J.* 59(8): 85(1976).
3. Baum, G. A., Brennan, D. C., and Habeger, C. C., *Tappi J.* 64(8): 97(1981).
4. Caulfield, D. F. and Weatherwax, R. C., in *Fibre-Water Interactions in Paper-making*, Vol. 2, British Paper and Board Industry Federation (Tech. Div.), London, 1978, pp. 741-58.
5. Nissan, A. H., in *Fibre-Water Interactions in Paper-making*, Vol. 2, British Paper and Board Industry Federation (Tech. Div.), London, 1978, pp. 609-29.
6. Zauscher, S., Nissan, A. H., and Caulfield, D. F., *TAPPI J.* 79(12): 178(1996).
7. Nissan, A. H., *Trans. Faraday Soc.* 53: 700(1957).
8. Nissan, A. H., Byrd, V. L., Batten, G. L., et al., *Tappi J.* 68(9): 118(1985).
9. Batten, G. L. and Nissan, A. H., *Tappi J.* 70(9): 119(1987).
10. Nordvall, E., "Ultrajudmätning av dragstyvhetsindex," thesis, Institute for Paper Technology, Royal Technical University, Stockholm, 1992.
11. Nielsen, L. F. and Landel, R. F., *Mechanical Properties of Polymers and Composites*, Marcel Dekker, New York, 1994, pp. 194-97.
12. Berger, B. J., Habeger, C. C., and Pankonin, B. M., *JPPS* 15(5): 170(1989).
13. Bradley, S. A. and Carr, S. H., *J. Polymer Sci. (Polymer Phys. Ed.)* 14: 111(1976).
14. Salmén, L., in *Products of Papermaking*, Vol. 1 (C. F. Baker, Ed.), PIRA, Leatherhead, UK, 1993.
15. Batten, G. L., in *Materials Interactions Relevant to the Pulp, Paper, and Wood Industries* (D. F. Caulfield, J. D. Passaretti, and S. F. Sobczynski, Eds.), MRS Symposium Proceedings, Vol. 197, Materials Research Society, Pittsburgh, 1990, pp. 163-72.
16. Htun, M. and Fellers, C., *Tappi J.* 65(4): 113(1982).
17. Batten, G. L. and Nissan, A. H., *Tappi J.* 69(10): 130(1986).
18. Batten, G. L. and Nissan, A. H., *Tappi J.* 70(11): 137(1987).
19. Perkins, R. W. and Mark, R. E., *The Role of Fundamental Research in Paper Making* (J. Brander, Ed.), Mechanical Engineering Publications, London, 1983, p. 479.
20. Bristow, J. A., Htun, M., Fellers, C., et al., *Tappi J.* 70(8): 115(1987).
21. Batten, G. L. and Nissan, A. H., *Tappi J.* 70(8): 117(1987).
22. Urbanik, T. J., *Tappi J.* 65(4): 104(1982).

APPENDIX

The Appendix consists of ten tables (Tables A-I-A-X) that present the detailed calculations for Sets 1-4 on Paper 11 (89.1-g/m² linerboard from pine sulfate pulp) of Nordvall (10). The same calculations were applied to data for all of the other sheets in the data set. Complete data for all 24 papers are available from the authors on request.

NOMENCLATURE

Variables

- ρ = apparent density of the paper at time of test, kg/m³
- A = intercept of $\ln E$ vs. w on the $\ln E$ ordinate
- a_1 = function of the anisotropy ratio r
- CI = cooperative index
- c_p = specific heat capacity at constant pressure (J/mole K)
- d = fiber-orientation correction factor
- D = intercept at zero water content from regression analysis of $\ln E$ vs. w in Regime II
- E = modulus of elasticity, N/m²
- E^* = specific modulus of elasticity, N·m/kg

- E_{tri} = quasi-static modulus of elasticity obtained by triangulation
- E_{urb} = quasi-static modulus of elasticity obtained by Urbanik's method, N/m² (22)
- k_R = force constant for stretching the H-bond, N/m
- n_e = total number of effective H-bonds per unit volume, 1/m³
- n_{equ} = total number of equivalent, effective H-bonds per unit volume, 1/m³
- p = probability value
- r = anisotropy ratio (E_{MD}/E_{CD})
- R_0 = H-bond length at equilibrium, m
- r^2 = correlation coefficient
- RH = relative humidity, %

- T_g = glass transition temperature, °C
- w = water content, mass of water per unit mass of paper
- w_c = critical water content

Subscripts

- 0 = zero moisture content
- iso = isotropic (i.e., invariant) modulus of elasticity
- s = quasi-static measurements
- u = ultrasonic measurements

Superscripts

- I = Regime I
- II = Regime II